EUROPEAN COOPERATION
IN THE FIELD OF SCIENTIFIC
AND TECHNICAL RESEARCH

EURO-COST

SOURCE: Centre for Communications Research
University of Bristol

COST 273 TD(05)115
Lisbon, Portugal
November 10-11, 2005

Channel Characterisation for Personal Area Networks

Dries Neirynck, Chris Williams, Andrew Nix and Mark Beach
Centre for Communications Research
Merchant Venturers Building
University of Bristol
Bristol, BS8 1UB, UK
Phone: +44 117 954 5123
Fax: +44 117 954 5206
Email: dries.neirynck@bristol.ac.uk

Channel Characterisation for Personal Area Networks

Dries Neirynck, Chris Williams, Andrew Nix and Mark Beach

Centre for Communications Research
Merchant Venturers Building
University of Bristol
Bristol, BS8 1UB, UK
dries.neirynck@bristol.ac.uk

Abstract

This paper presents channel characterisation work carried out at the University of Bristol as part of the Mobile VCE Core 3 programme. Three major measurement campaigns have been conducted. The first is focused on SISO links in body area networks (BAN). Particular attention is given to the relationship between the channel characteristics and the user's motion. The second set of measurements investigates the potential of multiple-input, multiple-output (MIMO) antenna systems in personal area networks (PAN). Finally, PAN MIMO measurements are conducted in an office environment.

I. Introduction

At the start of the Mobile VCE Core 3 programme in October 2002, the personal area network concept was growing in importance. However, very little was known about the type of channel conditions that could be expected. In order to address this lack of knowledge, the Core 3 programme included significant channel characterisation, some of which is presented in this paper.

The first measurment campaign, reported in section II, extends existing work on SISO channel measurements. Section III reports on initial investigations into the use of MIMO in a personal area network environment. These are followed by results from a MIMO measurement campaign using distributed antennas in a PAN scenario. The final section contains an overview of the main conclusions.

II. SISO in BAN

It is well-known that the proximity of the user will change the antenna characteristics (e.g. [1], [2]). In some studies, the influence of the user on the narrowband propagation characteristics for a terminal to access point link have been measured (e.g. [3], [4]). Hall *et al.* were, to our knowledge, the only group that had carried out narrowband propagation measurements between two on-body locations (shoulder to hip) [5], [6]. It was shown that significant channel loss variations occur and that these are related to the user's behaviour. This section presents the results from a wideband extension to this work that includes several additional on-body locations and was performed using ultra-wideband antennas in order to allow instantaneous comparisons between frequency bands.

The work reported in this paper has formed part of the Wireless Enablers work area of the Core 3 Research Programme of the Virtual Centre of Excellence in Mobile & Personal Communications, Mobile VCE, www.mobilevce.com, whose funding support, including that of EPSRC, is gratefully acknowledged. Fully detailed technical reports on this research are available to Industrial Members of Mobile VCE.

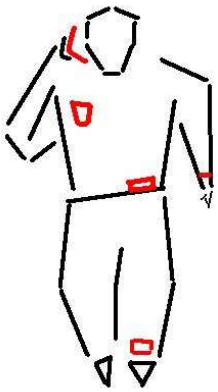

Next to head, right-hand side
Chest Pocket, right-hand side
Back Pocket Waist, left-hand side
Wrist, left-hand side
Ankle, left-hand side

Fig. 1. On-body antenna locations

A. Measurements

For the results presented here, wideband channel[1] frequency responses were measured by recording the forward transmission coefficients, S_{21}, between two ultrawideband antennas with a network analyser at frequencies spaced 1 MHz apart. Selected measurements were repeated at a later date using a Medav channel sounder and directional patch antennas [7].

The ultra-wideband (UWB) antennas were taken from the Time Domain PulsON 200 Ultra-Wide Band Evaluation Kit [8]. The use of UWB antennas allows for simultaneous recording of the channel in both the 2.4 and 5.2 GHz unlicensed frequency bands with similar antenna patterns. Characterisation in the anechoic chamber has revealed that the antennas are omni-directional. During the measurements, the antennas were placed at five on-body locations, listed in table 1.

The measurements took place at a variety of indoor locations, one outdoor location and in an anechoic chamber, with the user either standing, sitting or walking around. For those measurements including an antenna on the wrist, the user's arm was swinging from behind the back to in front of the chest.

B. Post-processing results

During post-processing of the measurements, the dynamics of the channel characteristics were studied. Figure 2 shows the variations in the channel loss for a link between chest and wrist recorded in the atrium of the University of Bristol's Merchant Venturers Building. The gaps between the responses represent the time the network analyser requires to write the results from its internal memory to the hard disk. As can be seen, there are rapid and significant changes in the received power in both frequency bands. Within a couple of seconds, the signal strength experiences 30 dB variations, which in the anechoic chamber increases to over 40 dB.

Similar variability was also observed in the RMS delay spread and the Ricean K-factor. The latter was estimated using the moment-based method [9], while the former was calculated from the power delay profile, after applying a 20 dB power window and taking into account the Hamming window used for the IFFT [10]. Figure 3 shows that there tends to be a relationship between the channel loss and the RMS delay spread. When the received power is high, the RMS delay spread is very low, while higher

[1]Since it is not feasible to accurately monitor the user's movements and the resulting changes to the antenna pattern and orientation, in this paper, the term "channel" will refer to the composite channel as perceived by the radio system, consisting of the actual radio channel and the user effects including changes to the antenna characteristics.

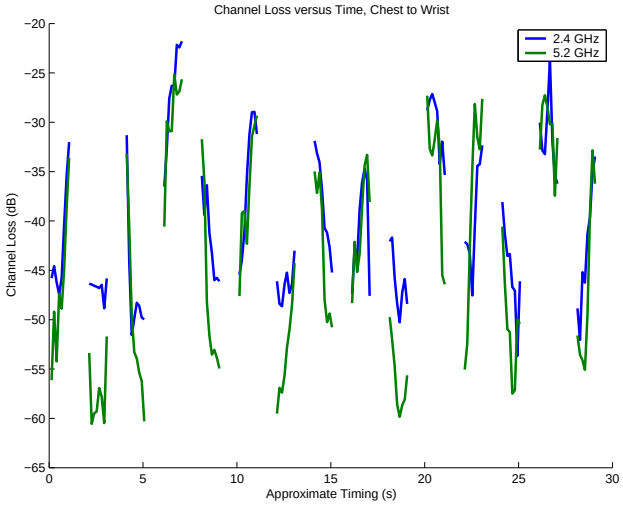

Fig. 2. Channel loss versus time, chest to wrist, standing with swinging arm, comparing frequency bands

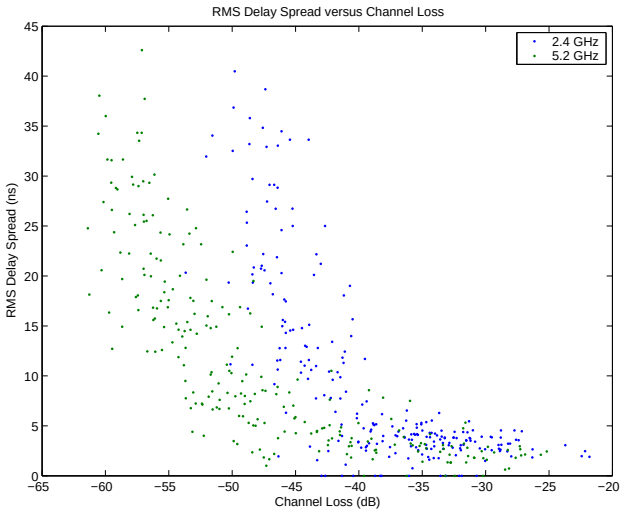

Fig. 3. Chest to wrist, standing with swinging arm, comparing frequency bands

RMS delay spreads correspond to lower received energy. The Ricean K-factor , on the other hand, is high when the received signal power is high and low when little energy is received.

Comparison with the measurements in the anechoic chamber explains these results. When the user's body obstructs the line-of-sight, the attenuation by the body is so high that the link relies on multipath in the environment. Hence, the RMS delay spread is higher while the Ricean K-factor decreases. Due to the short distance between the antennas, when the line of sight is present, the received power and K-factor will be high while the RMS delay spreads drop to (almost) zero. The dependence of the channel characteristics on the line-of-sight explains why, in figure 4, the channel characteristics of the other antenna locations are a subset of those from the chest to wrist link.

As fig. 4 demonstrates, the link between the chest and the wrist of the swinging arm is an extreme case. To get a feel of the coherence times of the coherence times during various user actions, we can use the measurements of [7].

It can be expected that the link between chest and wrist will be most variable in the case of the swinging

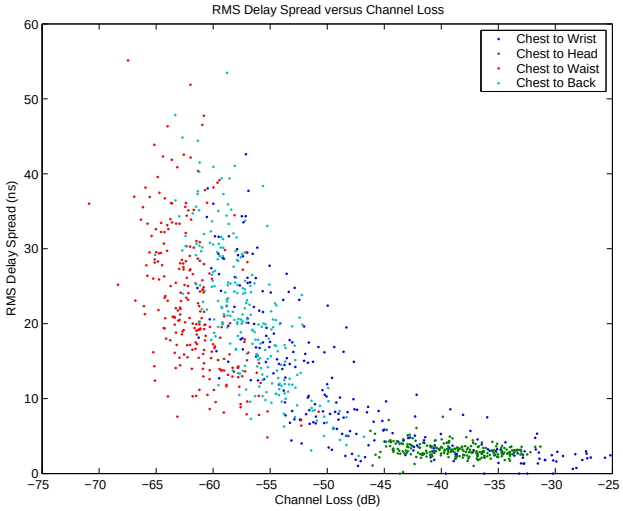

Fig. 4. Transmitting from chest, standing with swinging arm, comparing receive locations, 5.2 GHz band

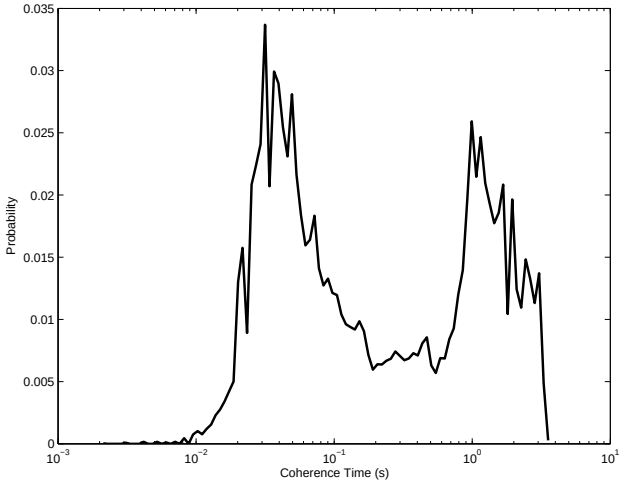

Fig. 5. PDF coherence times, chest to wrist

arm used above. Fig. 5 shows the pdf of the coherence times for the same link in the measurements from [7]. Here, the person carrying the antennas was performing a routine consisting of sitting, moving to standing, marching on the spot, turning to the left, then to the right and finally bending forward and standing up again. Each action was performed for about five seconds, resulting in a 30-second routine.

The coherence time is calculated as the time period where the complex correlation coefficients between the wideband frequency responses with the current frequency response are higher than 0.9. The resolution of the calculation is limited by the 1.024 ms spacing of channel snapshots. Analysis of the results shows that the coherence time is most likely to be either short (a few tens of milliseconds) during periods of movement or long (in the order of a second in this measurement) during the quieter periods of the routine.

It was therefore concluded that the channel conditions in the body area network are not as benign as the short distance between the transmitter and receiver suggests. Signal attenuation due to body blocking is high and when present will force the link to rely on multipath propagation in the environment. Furthermore, user actions can change the channel characteristics radically in very short periods of time.

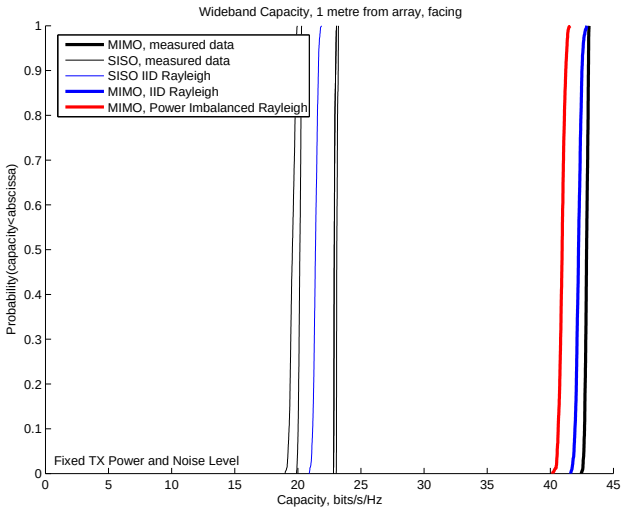

Fig. 6. Wideband Capacity Comparison

Both effects have been observed in both frequency bands under test.

III. MIMO IN PAN

It is well-known that in uncorrelated fading channels MIMO results in high capacity [11]. Because of the likely presence of a line-of-sight path in PAN communication links, and the resulting correlation between sub-channels, it is often assumed that MIMO is not appropriate for this application. In this section, a measurement campaign investigating the use of spatial diversity in a PAN scenario is reported.

A. Measurements

The results presented are based on measurements that took place in a small room (5 by 4 metres); part of the Wireless and Networks Research Lab on level 1 of the University of Bristol's Merchant Venturers Building (UK). Apart from two people, the measurement equipment and some furniture, the room was empty. One of the two persons present had two, transmitting, stacked patch antennas [12] mounted at chest height. These represent devices in a chest pocket or antennas integrated into the user's clothing and have therefore been spaced 15 cm apart. The user faced the array and stood at a separation distance of around 1 metre. The receiving array was an eight plus two passive element 5.2 GHz uniform linear array with half wavelength antenna spacing. For the 2-by-2 MIMO system evaluation reported below, antenna elements 1 and 7 are used.

B. Post-Processing Results

Fig. 6 compares the wideband capacities of the measured SISO and MIMO links with equivalent independent, identically distributed (IID) Rayleigh channels. In order to do this, the capacity was averaged over the 120 MHz measurement bandwidth.

The differences between the SISO capacities are due to a gain imbalance caused by body mounting, which results in antenna orientation and polarisation alignment differences. In the measured data, up to 10 dB of power difference is observed between the elements. Therefore, to aid comparison, fig. 6 also includes the capacity of an equivalent MIMO system with Rayleigh fading channels that have the same power imbalance as the measured channels.

Despite the power imbalance and the clear line-of-sight, the measured channels outperform both the IID and power imbalanced Rayleigh fading MIMO systems. This is due to the deterministic effect of the LOS. Since there is no fading, the capacity is constant over the measurement bandwidth and time

period, while the Rayleigh wideband average is taken over a number of narrowband frequency bins that fade arbitrarily. For the measurements presented here, the measured data has a capacity equal to that of the highest narrowband Rayleigh fading channels over the whole measurement bandwidth.

The latter is still surprising because it is well known that uncorrelated channels result in high MIMO capacity. Since the system is operating in line-of-sight and at short-range, it is unlikely that scatterers provide the necessary decorrelation. Indeed, analysis of the correlation coefficients shows that they all fall on the unit circle.

C. Analysis

As the measurement results demonstrate, high correlation coefficients do not necessarily lead to low MIMO capacity. In the narrowband case, the capacity equation is given by [11]:

$$C = log_2\left[det\left[I_{N_R} + \frac{\rho}{N_T} HH^{\dagger}\right]\right] \quad bps/Hz \tag{1}$$

Hence, the capacity is determined by the properties of $HH^{\dagger}$, which, for 2-by-2 MIMO, can be extended as[2]:

$$\begin{aligned} HH^{\dagger} &= \begin{bmatrix} h_{11} & h_{12} \\ h_{21} & h_{22} \end{bmatrix} \begin{bmatrix} h'_{11} & h'_{21} \\ h'_{12} & h'_{22} \end{bmatrix} \\ &= \begin{bmatrix} h_{11}h'_{11} + h_{12}h'_{12} & h_{11}h'_{21} + h_{12}h'_{22} \\ h_{21}h'_{11} + h_{22}h'_{12} & h_{21}h'_{21} + h_{22}h'_{22} \end{bmatrix} \end{aligned} \tag{2}$$

The entries on the diagonal will be real valued and equal to the sum of the power of the respective channels. For a particular location, this will be dependent on the path loss. The value of the determinant, and hence the MIMO capacity, is determined by the sum of $h_{21}h'_{11}$ and $h_{22}h'_{12}$. The capacity will be maximal when these off-diagonal values are zero. Since $h_{21}h'_{11} + h_{22}h'_{12}$ is the inner product of the rows of H, maximal capacity is achieved when the channel matrix H is orthogonal [13].

Note that $h_x h'_y$ is proportional to the correlation coefficient. In most scenarios, the channel coefficients are out of the designer's control and hence uncorrelated scattering is required to minimise the values of the off-diagonal entries. In pure LOS, however, the channel coefficients become deterministic. The phase difference between the channel coefficients is fixed and dependent on the operating frequency, array geometry and positions [14]. Since the coefficients are complex valued, even highly correlated channel coefficients can add destructively, and result in orthogonal rows. In order for this to happen, a significant phase difference between the channel coefficients is required. This is possible when the spherical nature of the wavefronts has to be taken into account, i.e. for systems operating over a short distance or with significant antenna spacings [15]. In [16], this has been used to derive a design criterion that maximises the channel capacity under LOS conditions.

The following normalised, LOS channel matrix will be used to generate an appreciation of the sensitivity of the capacity to orthogonality:

$$H = \begin{bmatrix} e^{-jkd_{11}} & e^{-jkd_{12}} \\ e^{-jkd_{21}} & e^{-jkd_{22}} \end{bmatrix}$$

where d_{xy} is the distance between transmit and receive antennas y and x. It is assumed that this distance is such that the path loss differences are negligible. As shown in [16], in this case, $HH^{\dagger}$ equals:

$$HH^{\dagger} = \begin{bmatrix} 2 & e^{jk(d_{21}-d_{11})} + e^{jk(d_{22}-d_{12})} \\ e^{jk(d_{11}-d_{21})} + e^{jk(d_{12}-d_{22})} & 2 \end{bmatrix}$$

[2]In this paper, † will be used to indicate the Hermitian of a matrix, while $'$ is used to indicate the complex conjugate of a number

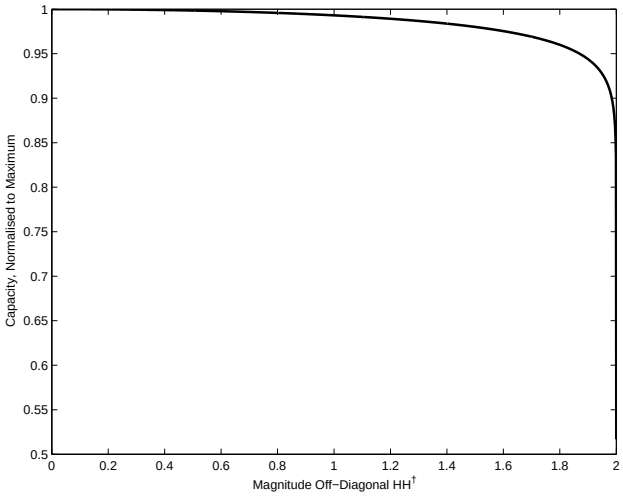

Fig. 7. Relation between orthogonality and capacity

where the magnitude of the off-diagonal sum varies between 0 and 2 depending on the antenna spacing. Since the entries on the diagonal are constant, the magnitude of the off-diagonal entry is a measure of the orthogonality of the channel matrix. The closer to zero, the closer to orthogonal the rows of the matrix, and the higher the system capacity. The exact relationship between this value and the resulting capacity for a system operating in the high SNR region is given in fig. 7. Due to the logarithmic relation between the two, the magnitude of the off-diagonal entries must rise up to 1.98 for the capacity to drop below 90 percent of its maximum value.

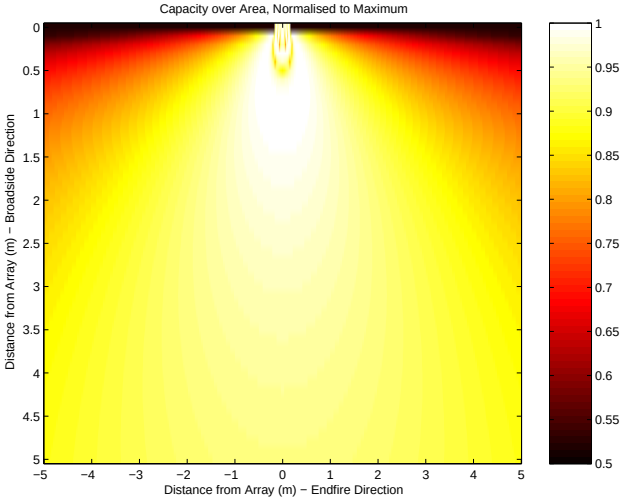

Fig. 8. Capacity in area in front of array

Therefore, a MIMO system can still offer significant capacity increases in LOS even if the conditions are not ideal. Indeed, in the recorded channels, 2-by-2 MIMO achieves an 85 percent capacity increase compared to a SISO system, not withstanding the 10 dB gain imbalance. In fig. 8, the capacity achieved by a 5.2 GHz MIMO system optimised for a separation distance of 1 metre is shown over an area of 10-by-5 metres. As can be seen, the MIMO system is able to extract a significant capacity increase in most of regions.

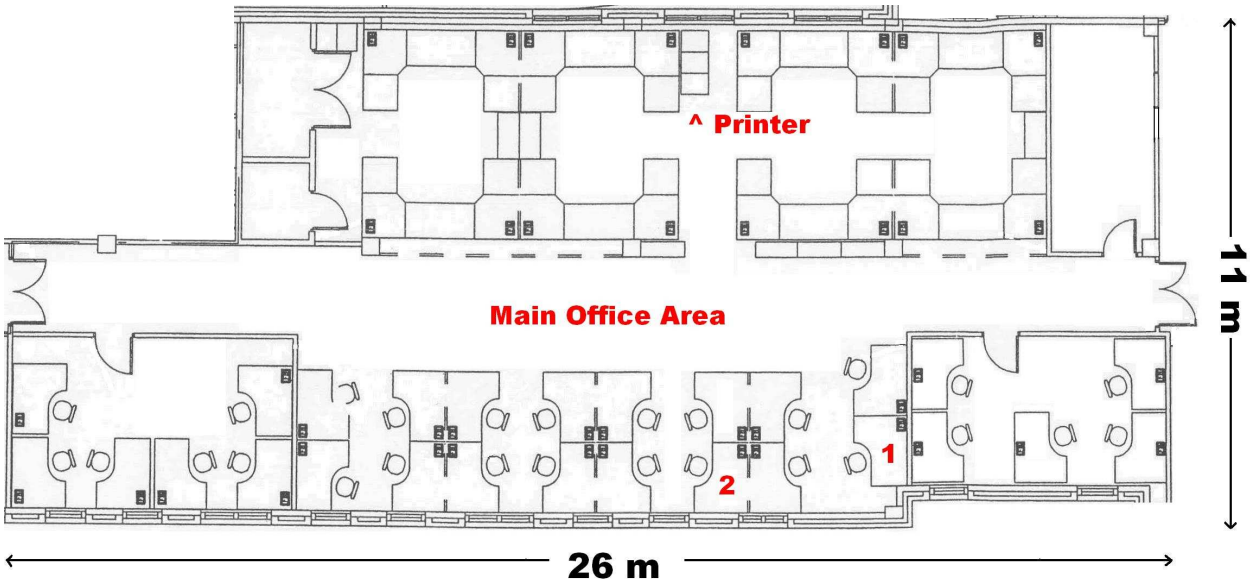

Fig. 9. Ground plan measurement environment

IV. MIMO IN OFFICE ENVIRONMENT PAN

A final measurement campaign was conducted in an office environment. The aim was to capture a channel data in a real environment that could be used for many purposes, including the characterisation of interference levels, co-operation between devices and the use of MIMO.

A. Measurements

These measurements have been carried out in the main office area of the Wireless and Networks Research Lab on level 1 of the University of Bristol's Merchant Venturers Building (UK). A ground plan can be found in fig. 9.

In this office, four antenna locations have been chosen. A uniform linear array has been mounted at the location of the printer. Two desks, number 1 and 2 in the figure, each have a group of four antennas distributed around them: 2 as a uniform linear array on the desktop, 1 on the screen and 1 lying on a near-by filing cabinet. A final four antennas are body-mounted, one pair on the front of the user, one pair at the back, both at chest height and spaced 15 cm apart. The person carrying the antennas is walking in the aisle of desk 2.

In order to be able to use the measurement data for the characterisation of interference and co-operation between devices, ideally, all channels between all antennas are measured as simultaneously as possible. The channel sounder, Medav RUSK BRI, uses fast multiplex boxes to switch between the various subchannels. However, it can only cope with dedicated transmit and receive antennas and records all channels in one snapshot with the same automatic gain control (AGC) setting. Therefore, it was decided that the antennas around the desks act as receivers, while the on-body antennas and the printer array act as transmitters.

In order to measure each group of antennas with the optimal AGC value, extra control circuitry was designed to select the transmitting and receiving group using the most significant bit of the multiplexer's control signal. One of the transmitting antenna ports was terminated with 50Ω, which allows to separate the measurements per link and will be used to determine the channel sounder's noisefloor.

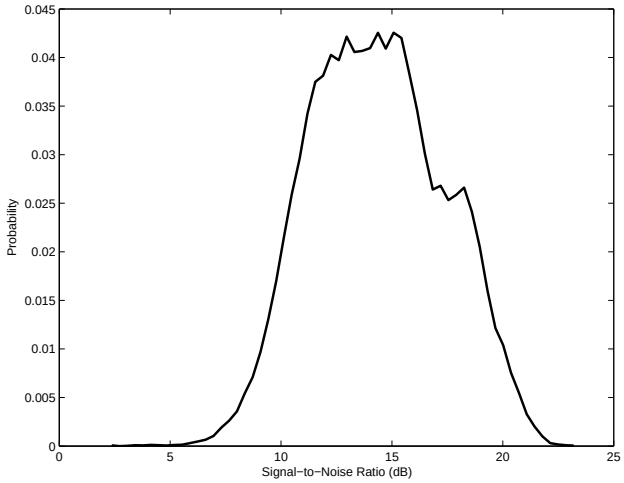

Fig. 10. Signal-to-noise ratio during measurements

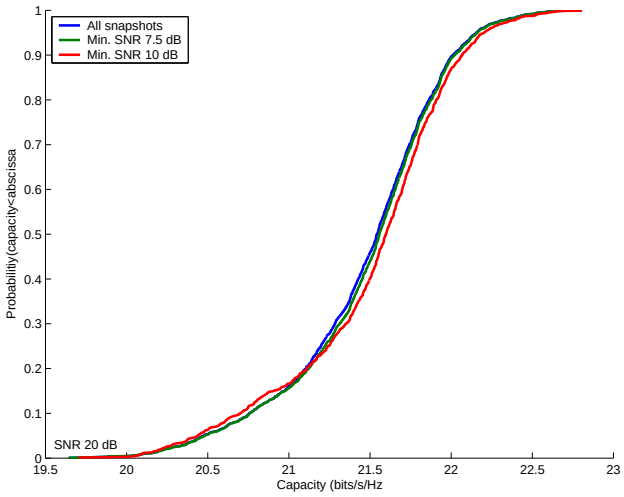

Fig. 11. CDF capacity with various imposed minimum measurement SNR

B. Post-processing results

Because of the distributed nature of the antenna “arrays”, the validity of the measured signals has been verified. The noise floor of the channel sounder was calculated as the average power recorded when the port with the 50Ω termination was active. Using this value, the signal-to-noise ratio of the measured data could be determined. Fig. 10 shows that this SNR can reach quite low values, below 5 dB.

In order to investigate the consequences of this, fig. 11 compares the CDFs of the capacity when various minimum signal-to-noise ratios are imposed. As can be seen, there is only a slight difference between the curves. Therefore, all measurements have been included in the analysis presented in the rest of this section.

Fig. 12 shows the PDF of the coherence times for the individual SISO links in the measurement files. The coherence time is calculated as the time period where the magnitude of the complex correlation coefficients between the wideband frequency responses with the current frequency response are higher than 0.9. Since the separation between the snapshots in the measurement file is 106.496 ms, this limits the resolution of the calculation and the coherence times are rounded to the first lower multiple of this

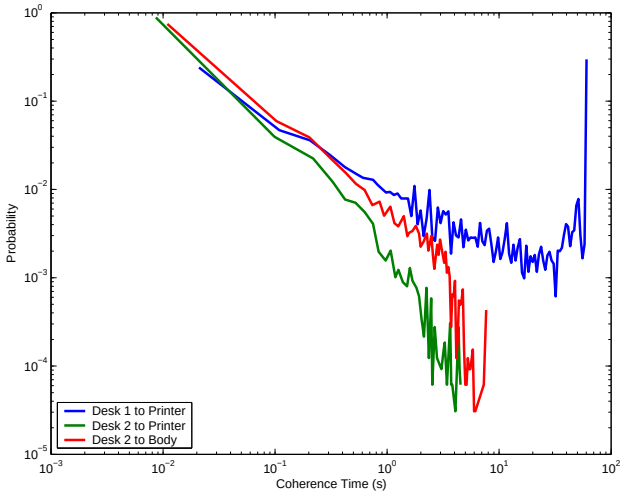

Fig. 12. PDF coherence times office environment

value. For those links where there was a poor measured signal-to-noise ratio, this could result in an underestimation of the coherence time. However, because of the already poor resolution and the fact that excluding snapshots would further limit the maximum coherence time, all snapshots have been used in the calculations.

As can be seen from the links between desk 1 and the printer, without direct human interaction, the channel hardly changes over the one minute long measurement period. The coherence times for the channels between desk 2 and the printer are being interrupted by the walking person. In most cases, this results in coherence times less than the resovable 106 ms. The coherence times between desk 2 and the walking person are slightly higher. Those channels that have a line of sight with the receiver result in longer coherence times.

Fig. 13 compares the link capacity between the body and desk 2 using various diversity schemes when walking in the aisle of desk 2. The SISO reference has been calculated using the vertical polarisations of antennas 1 on the desktop and the user. For polarisation diversity, this is combined with the horizontal polarisations of the same antennas; while for space diversity, the vertical polarisation of the other antenna on the desktop and the front of the user are used. Combined space and polarisation diversity is achieved by combining with the horizontal polarisation of the other antenna. The capacities were calculated assuming a fixed transmit power (10 dBm) and noise floor (-80 dBm) and averaged over the 120 MHz measurement bandwidth.

All diversity schemes result in significant capacity increases, close to twice the SISO capacity. In most cases, and as demonstrated by the particular measurement used for fig. 13, no significant differences between the various diversity mechanisms have been observed.

V. Conclusions

This paper has presented channel characterisation work for body and personal area networks. The determining influence of the user on the SISO channel characterstics in the 2.4 and 5.2 GHz unlicensed frequency bands have been demonstrated and discussed. Two measurement campaigns focusing on the use of MIMO in PAN have been presented. It was shown how spatial diversity in PAN can be obtained and results from an office-based measurement campaign were included.

VI. Acknowledgements

The authors are very grateful for the guidance from the Industrial Members of the Mobile VCE Wireless Enablers Steering Group and would like to express particular thanks to Dr. Dean Kitchener from Nortel

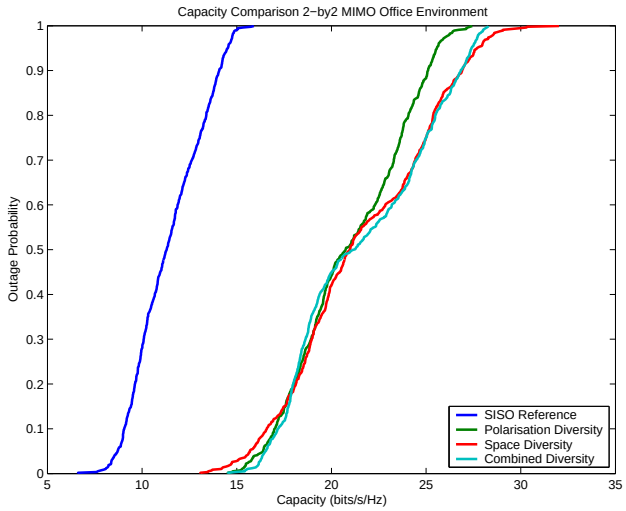

Fig. 13. Comparison diversity mechanisms MIMO, desk 2 to body, walking around

Wireless Technology Laboratories UK.

REFERENCES

[1] K. Meksamoot, M. Krairiksh, and J. ichi Takada, "A polarization diversity PIFA on portable telephone and the human body effects on its performance," *IEICE Trans. Commun.*, vol. E84-B, pp. 2460 – 2467, Sept. 2001.

[2] F.-L. Lin and H.-R. Chuang, "Performance evaluation of a portable radio close to the operator's body in urban mobile environments," *IEEE Transactions on Vehicular Technology*, vol. 49, pp. 614 – 621, Mar. 2000.

[3] K. Ziri-Castro, W. Scanlon, R. Feustle, and N. Evans, "Channel modelling and propagation measurements for a bodyworn 5.2 ghz terminal moving in the indoor environment," *12th IEE Intl. Conf. Antennas & Propagation (IEE Conf. Publ. No. 491)*, vol. 1, pp. 67–70, Apr. 2003.

[4] J. O. Nielsen, G. F. Pedersen, K. Olesen, and I. Z. Kovács, "Statistics of measured body loss for mobile phones," *IEEE Transactions on Antennas and Propagation*, vol. 49, pp. 1351–1353, Sept. 2001.

[5] P. Hall, M. Ricci, and D. H. T. Wei, "Characterization of on-body communication channels," *3rd International Conference on Microwave and Millimeter Wave Technology Proceedings, Beijing, China*, pp. 770 – 772, Aug. 2002.

[6] T. H. PS Hall, M Ricci, "Measurements of on-body propagation characteristics," *Proceedings of the IEEE Antennas and Propagation Society International Symposium, San Antonio*, pp. 310–313, 2002.

[7] R. Smerin, "Channel modelling for body area networks," M.Eng. Dissertation, University of Bristol, Apr. 2005.

[8] Time domain corporation. [Online]. Available: http://www.timedomain.com/products/pulson.html

[9] L. Greenstein, D. Michelson, and V. Erceg, "Moment-method estimation of the ricean k-factor," *IEEE Communications Letters*, vol. 3, no. 6, pp. 175–176, June 1999.

[10] A. Saleh and R. Valenzuela, "A statistical model for indoor multipath propagation," *IEEE Journal on Selected Areas in Communications*, vol. 5, pp. 128 – 137, Feb. 1987.

[11] G. Foschini and M. Gans, "On limits of wireless communications in a fading environment when using multiple antennas," *Wireless Personal Communications*, vol. 6, pp. 331–335, 1998.

[12] D. L. Paul, I. J. Craddock, C. J. Railton, P. N. Fletcher, and M. Dean, "FDTD analysis and design of probe-fed dual-polarized circular stacked patch antenna," *Microwave and Optical Technology Letters*, vol. 29, no. 4, pp. 223–226, May 2001.

[13] D. Gesbert, H. Bölcskei, D. A. Gore, and A. J. Paulraj, "Outdoor MIMO wireless channels: Models and performance prediction," *IEEE Transactions on Communications*, vol. 50, no. 12, pp. 1926–1934, Dec. 2002.

[14] P. Driessen and G. Foschini, "On the capacity formula for multiple input - multiple output wireless channels: A geometric interpretation," *IEEE Transactions on Communications*, vol. 47, no. 2, pp. 173–176, Feb. 1999.

[15] J.-S. Jiang and M. A. Ingram, "Distributed source model for short-range MIMO," in *IEEE 58th Vehicular Technology Conference, VTC 2003-Fall*, vol. 1, Oct. 2003, pp. 357–362.

[16] I. Sarris and A. Nix, "Maximum MIMO capacity in line-of-sight," in *International Conference on Information, Communications and Signal Processing*, 2005, In Press.